社団法人　電子情報通信学会
THE INSTITUTE OF ELECTRONICS,
INFORMATION AND COMMUNICATION ENGINEERS

信学技報
TECHNICAL REPORT OF IEICE.

生物共生モデルにもとづくパス／パケット光統合ネットワークの動的リソース制御手法の提案と評価

荒川　伸一† 　筒井　宣充† 　村田　正幸†

† 大阪大学　大学院情報科学研究科　〒 565-0871 大阪府吹田市山田丘 1-5
E-mail: †{arakawa,n-tsutsui,murata}@ist.osaka-u.ac.jp

あらまし　本稿では，パケット交換ネットワークとパス交換ネットワークに対してそれぞれ波長を割当てることで構築するパケット・パス統合ネットワークを対象とし，ネットワークの状況の変化に対して適応的に波長リソースを割り当てる動的波長割当手法を提案する．提案手法は，細胞膜と培地を介した代謝物の交換によって二種のバクテリアが共生する仕組みを説明する数学モデルの生物共生モデルにもとづいており，お互いのネットワークのスループットを高めつつ，共生を図るものである．計算機シミュレーションにより，閾値をもとに波長リソースを割り当てる手法と比較して，データ転送が完了するまでの時間が 40% 程度低減することを示す．

キーワード　パス / パケット統合ネットワーク，IP over WDM，波長ルーティング，TCP, レイテンシ

A Biologically-inspired Wavelength Allocation Method for Optical Path/Packet Integrated Networks

Shin'ichi ARAKAWA†, Norimitsu TSUTSUI†, and Masayuki MURATA†

† Graduate School of Information Science and Technology, Osaka University
Yamadaoka 1-5, Suita, Osaka, 565-0871 Japan
E-mail: †{arakawa,n-tsutsui,murata}@ist.osaka-u.ac.jp

Abstract　In this paper, we develop a biologically-inspired wavelength allocation method that allocates wavelengths to path/packet integrated networks. Our method is based on a biological symbiosis model that explains co-existing and co-working of two types of bacterial strains in biological systems. The results show that biologically-inspired wavelength allocation method achieves a nealy 40% reduction of the latency from threshold-based dynamic wavelength allocation method.

Key words　path/packet integration, IP over WDM, circuit switching, wavelength routing, Transmission Control Protocol (TCP), latency

1. Introduction

To effectively utilizing the wavelength-routing capability in a WDM-based optical networks, two approaches have been investigated [1, 2]. One of approaches is to transfer the data based on the circuit-switching paradigm. That is, when a data transfer request arises at a source node, a wavelength is dynamically reserved between the source and destination nodes and a lightpath is configured. Then, the data is transferred using the allocated wavelength channel. After the data transmission using the lightpath, the lightpath is immediately released. Another approach is called IP-packet over WDM [2] where a data is transferred based on packet switching paradigm. In this approach, each node consists of IP router and OXC (Optical Cross Connect) that binds an input wavelength channel to a specified output wavelength channel. Then, a virtual network topology (VNT) is constructed in advance by setting up lightpaths between two IP routers. The lightpath behaves as the virtual link from viewpoint of IP networks. Then, a data transfer is performed based on the packet switching paradigm over the VNT.

The main strength of the circuit-switching paradigm is the data request solely uses and enjoys the bandwidth of wavelength channels, which would be attractive for recent multimedia services and/or cloud services that require high reliability and large bandwidth. Another strength is that a congestion avoidance mechanism is no longer necessary. That is, any transport protocols other than TCP can be used for the data transfer. In a recent study, a transport protocol that effectively utilizes the wavelength channel is investigated in Ref. [3]. The drawbacks of this approach are the lightpath setup delay, defined from when data transfer request arises to time when data transfer starts, and blocking during the lightpath establishment.

The current Internet is mainly based on the packet switching paradigm. However, many problems arise with increasing traffic demand and advances of related networking technologies and networking services. For example, the packet drop rate and packet delay increases because of congestion caused by other user traffic [4], which is an inevitable characteristic and may be crucial for services requiring high reliability and large bandwidth. To relax this, over-provisioning of link capacity and router's processing capability are widely used. However, the over-provisioning is eventually difficult because of technological constraints, such as the limitation of packet processing speeds, and economical constraints, such as power-consumption for high-speed (and high-cost) packet processing interfaces. Although more advances of technologies may resolve the limitation of packet processing capacity and reduce the cost, the above-mentioned characteristics are essential for the packet-switching paradigm.

Thus, constructing only packet switched network or circuit switched network cannot satisfy requirements, such as the high reliability and large bandwidth, for future networking services. An integration of circuit switched network and packet switched network is required to enjoy strength of both circuit-switching paradigm and packet-switching paradigm. One possible approach to fulfill this is to deploy the WDM technology and allocate different wavelengths for each network. Hereafter, we will call a network based on the packet-switching paradigm as the packet-based network and call a network based on the circuit-switching paradigm as the path-based network.

We have investigated a performance of path/packet integrated networks in [5, 6]. Reference [5] evaluates the performance of path/packet integrated networks with respected to the network throughput, and show the advantage of path/packet integrated networks. The authors developed a numerical method that derive the network throughput with a fixed wavelength allocation for packet-based network and path-based network. Reference [6] demonstrated that the fixed wavelength allocation does not minimize the latency, which is defined from when a data transfer request arises to when the data transfer completes, when the network environments changes. The simulation results clearly showed that the optimal wavelength allocation depends on the arrival rate of data transfer requests, so the authors propose a dynamic wavelength allocation method that is based on a threshold of queue length of buffer in the packet-based network.

In this paper, we present another dynamic wavelength allocation method that is based on a biological symbiosis model developed in [7]. The biological symbiosis model is the mathmatical model that explains co-existing and co-working of two types of bacterial strains. By interpreting bacterial strains as the amount of traffic transfered by packet-switched / circuit-switched network, we achieve the co-existing and co-working of packet-switched / circuit-switched network against the changes of network conditions.

This paper is organized as follows. In Section 2, we introduce the network architecture of path/packet integrated networks. In Section 3, we explain our biologically-inspired wavelength allocation method. In Section 4, we evaluate their performance in path/packet integrated networks. Section 5 concludes this paper.

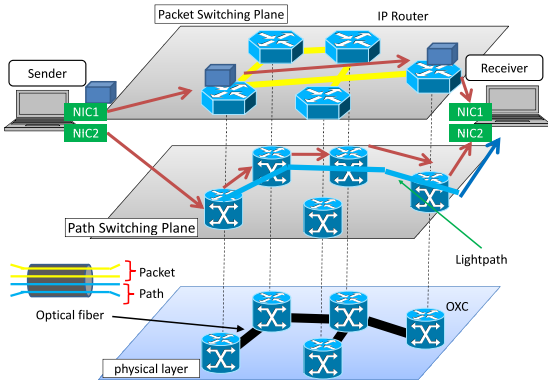

Figure 1 Network architecture

2. A model of path/packet integrated network

Each node in path/packet integrated network consists of IP router and OXC. OXCs are connected with optical fiber. The path/packet integrated network provides a packet switched network and a circuit switched network by allocating wavelengths for each network. For the packet switched network, the virtual network topology is constructed by pre-configuring a set of lightpaths. When a packet arrives at a node, the packet is forwarded to the next node in the VNT. In the circuit switched network, when a data transfer request arises, lightpaths are established between source and destination nodes on-demand basis (Figure 1). RSVP-based wavelength reservation protocol is used in this paper.

Each end-host connecting with the node has two network interfaces; one for forwarding IP packet via packet switched network and one for establishing a lightpath between two end-hosts. When the data transfer request arises, the end-host selects the packet switched network or the circuit switched network to transfer the data. Various strategies to select the network can be considered. We believe that the optimal strategy highly depends on the traffic characteristics, so the highly sophisticated strategy may be necessary. Instead of chasing the sophisticated strategy, we take a simple strategy to select the network because our primary concern of the current paper is to develop an adaptive wavelength allocation method. In this paper, the sender host first tries to transfer the data in circuit switched network. When the lightpath establishment succeeds, the sender host transfers the data using the maximum bandwidth of wavelengths. When the lightpath establishment fails, the sender host gives up transferring the data via circuit switched network and transfers the data via the packet switched network. In this case, the sender host uses TCP protocols during the data transfer.

We consider the dynamic wavelength allocation for packet-switched network and circuit-switched network. Its enabling architecture is illustrated in Figure 2. There is a controller to manage the configuration of OXCs and observe the network environment, such as the buffer utilization of IP routers, the blocking rate of lightpath establishments, and the packet dropped rate in the IP router. Depending on the wavelength methods explained in later, the controller collects the buffer utilization of IP router (in threshold-base wavelength allocation) or the blocking rate and the packet drop rate in the IP router (in biologically-inspired wavelength allocation). Then, for

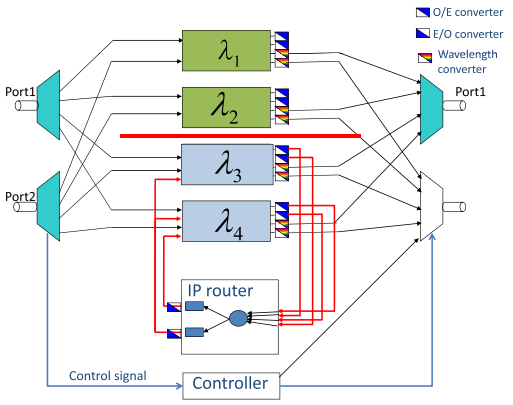

Figure 2 Node architecture for dynamic wavelength allocation: Focusing on the output port 1. Two wavelenghts are assigned for packet switching plane and path switching plane.

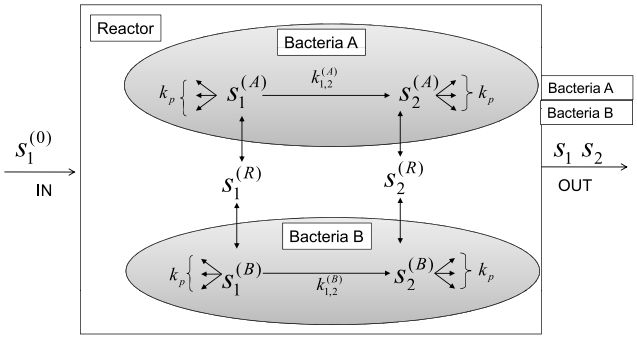

Figure 3 Biological symbiosis model

example, when the controller determines to increase the amount of wavelengths allocated to the path switching plane, the controller immediately reconfigure the optical switch for λ_3 so as not to forward the optical-signal to the IP router.

3. Biologically-inspired Wavelength Allocation Method for Optical Path/Packet Integrated Networks

3.1 Biological symbiosis model

In [7], the authors proposed a mathematical model of a mechanism that permitted two types of bacterial strains to live together by exchanging metabolites through a reactor. Bacterial strains have a metabolic network of generating metabolite S_2 from other metabolite S_1. Metabolites diffuse in and diffuse out of a cell through membrane depending on the difference in metabolic concentrations (Figure 3). The dynamics of concentrations of metabolites in a cell of strain A and B are formulated as,

$$ds_1^{(A)}/dt = (P/V)(s_1^{(R)} - s_1^{(A)}) - (k_{1,2}^{(A)} + k_p)s_1^{(A)}, \quad (1)$$
$$ds_1^{(B)}/dt = (P/V)(s_1^{(R)} - s_1^{(B)}) - (k_{1,2}^{(B)} + k_p)s_1^{(B)}, \quad (2)$$
$$ds_2^{(A)}/dt = (P/V)(s_2^{(R)} - s_2^{(A)}) + k_{1,2}^{(A)}s_1^{(A)} - k_p s_2^{(A)}, \quad (3)$$
$$ds_2^{(B)}/dt = (P/V)(s_2^{(R)} - s_2^{(B)}) + k_{1,2}^{(B)}s_1^{(B)} - k_p s_2^{(B)}, \quad (4)$$

where P stands for the permeation coefficient of cell membrane, V does for the average volume of a cell. $s_{1,2}^{(A)}$, $s_{1,2}^{(B)}$ and $s_{1,2}^{(R)}$ are metabolite concentrations in a cell of strain A and B in the reactor, respectively. k_p is the metabolite consumption rate in a cell. $k_{1,2}^{(A)}$ and $k_{1,2}^{(B)}$ are the metabolite conversion rate in a cell of strain A and B. Next, metabolite concentrations in the reactor evolve as,

$$ds_1^{(R)}/dt = D(s_1^{(0)} - s_1^{(R)}) + X^{(A)}P(s_1^{(A)} - s_1^{(R)}) + X^{(B)}P(s_1^{(B)} - s_1^{(R)}), \quad (5)$$
$$ds_2^{(R)}/dt = D(s_2^{(0)} - s_2^{(R)}) + X^{(A)}P(s_2^{(A)} - s_2^{(R)}) + X^{(B)}P(s_2^{(B)} - s_2^{(R)}), \quad (6)$$

where $X^{(A)}$ and $X^{(B)}$ stand for the number of cells of strain A and B per volume in the reactor. The fresh medium containing metabolites of concentration $s_1^{(0)}$ and $s_2^{(0)}$ are added to the reactor at the constant rate and the culture is drained at the same rate. D means the resultant dilution rate. Change in population of cells is formulated as,

$$dX^{(A)}/dt = u^{(A)}X^{(A)} - DX^{(A)}, \quad (7)$$
$$dX^{(B)}/dt = u^{(B)}X^{(B)} - DX^{(B)}, \quad (8)$$

where the growth rate $u^{(A)}$ and $u^{(B)}$ is defined as,

$$u^{(A)} = \alpha s_1^{(A)}s_2^{(A)}, \quad (9)$$
$$u^{(B)} = \alpha s_1^{(B)}s_2^{(B)}, \quad (10)$$

Eq. (9) implies that a cell with high metabolite concentration grows fast. Here, α (> 0) is a constant.

3.2 Applying the biological symbiosis model to dynamic wavelength allocation method

In this section, we explain how the biological symbiosis model can be applied to the wavelength allocation methods. More specifically, we describe how to determine the amount of wavelengths allocated for the packet switching plane and the path switching plane. Since the biological symbiosis model does not distinguish the role of A and B, we regard the bacteria A for the path switching plane and the bacteria B for the packet switching plane.

Table 1 is the correspondence table between parameters in biological symbiosis model and our wavelength allocation method. The number of bacteria A, $X^{(A)}$, represents number of wavelengths allocated to the path switching plane and the number of bacteria B, $X^{(B)}$, represents the number of wavelengths allocated to the packet switching plane. In calculating $X^{(A)}$ and $X^{(B)}$ from Equations 1-9, we need to specify definitions of $k_{1,2}^{(A)}$ and $k_{1,2}^{(B)}$ since they represent degree of productivity of the path switching plane and the packet switching plane. In our model, the degree of productivity is derived from the throughput of each plane, that is, $k_{1,2}^{(A)}$ and $k_{1,2}^{(B)}$ is calculated from following equations,

$$k_{1,2}^{(A)} = (1.0 - P_b) \cdot C, \quad (11)$$
$$k_{1,2}^{(B)} = (s/RTT) \cdot \sqrt{(3/2)} \cdot \sqrt{(1/p)}, \quad (12)$$

where P_b is the blocking rate of lightpath establishments on the path switching plane and C is the bandwidth of lightpaths (in [Gbps]). B is the packet size and RTT is the propagation delay of connections. p is the packet loss probability in the packet switching plane. β is the parameter that adjusts the throughput by [Gbps] and is set to 10^{-9}. Note that $k_{1,2}^{(B)}$ is TCP's throughput calculation formula and RTT should be determined by the observed round-trip time. However, in our simulation, RTT is set to the propagation delay because the queuing delay is relatively small in the WDM-based networks. In the realistic situation, we may need the RTT estimation at the controller in nodes [8].

Table 1 Correspondence table between parameters in biological symbiosis model and our dynamic wavelength allocation method

$X^{(A)}$	Number of wavelengths allocated to the path switching plane	$X^{(B)}$	Number of wavelengths allocated to the packet switching plane
$s_1^{(A)}$	Number of wavelengths allocated to the path switching plane per unit of time	$s_1^{(B)}$	Number of wavelengths allocated to the packet switching plane per unit of time
$s_2^{(A)}$	Throughput in the path switching plane per unit of time [Gbps]	$s_2^{(B)}$	Throughput in the packet switching plane per unit of time [Gbps]
$k_{1,2}^{(A)}$	Throughput of the path switching plane [Gbps]	$k_{1,2}^{(B)}$	Throughput of the packet switching plane [Gbps]
$u^{(A)}$	Growth rate of the path switching plane per unit of time	$u^{(B)}$	Growth rate of the packet switching plane per unit of time
$s_1^{(R)}$	Internal variable that represents the remaining wavelength resources that are not assigned to switching planes	$s_2^{(R)}$	Internal variable that represents throughput per unit of time [Gbps]
$s_1^{(0)}$	Number of wavelength multiplexed on a fiber	$s_2^{(0)}$	Parameter (set to 0)
$k^{(p)}$	Parameter	D	Parameter
P	Parameter	α	Parameter

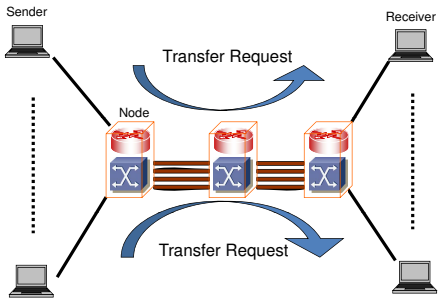

Figure 4 Dumbbell network

Table 2 Simulation parameters

OD pairs	120
OXC configuration delay	0 ms
Link propagation delay	10 ms
Arrival process	Poisson
Amount of data	Exponential distribution with mean 1 Gbit
Bandwidth of a wavelength	10 Gbps
Number of wavelengths	8
Buffer size at IP routers	256 MB

4. Evaluation

4.1 Simulation parameters

For our evaluation, we use the dumbbell network shown in Figure 4. The network has sender hosts and receiver hosts equipped with two network interfaces. Nodes, each having IP router and OXC, are connected with hosts via the network interfaces, and are also connected with each other via WDM transmission link. The number of wavelengths multiplexed between nodes is eight, and the buffer size of each IP router is 256MB. In this evaluation, we assume that the bandwidth of links between sender hosts and nodes is enough not to be a bottleneck of path/packet integrated networks.

In the packet switching plane, the packet is processed based on the FIFO (First-in First-out) drop-tail discipline. The sender host employs TCP Reno when the data is transferred via the packet switching plane. When the path switching plane is used, the sender host transfers the data with the maximum bandwidth of wavelengths since the sender host exclusively uses the lightpath. The other simulation parameters are summarized in Table 2 .

The performance metric used in this paper is the average latency. We define latency as the time from when a data transfer request arises to when the data transfer completes. The formal definition of the average latency is,

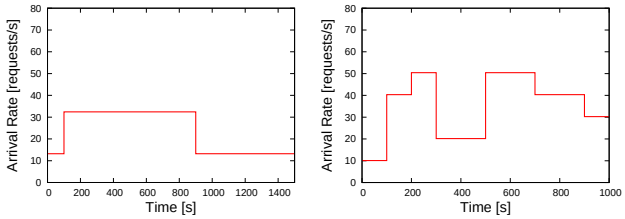

(a) Scenario 1 (b) Scenario 2

Figure 5 Time variation of arrival rate for two traffic scenarios

$$(\sum_{i=1}^{n_c} P_i + \sum_{k=1}^{n_p} B_k + \sum_{k=1}^{n_p} T_k)/(n_c + n_p), \tag{13}$$

where n_c is the number of data transfers completed by using the path switching plane and n_p is the number of data transfers completed by using the packet switching plane. P_i represents the latency of the i-th request among the n_c requests. For the k-th request among the n_p requests, we define B_k as the time consumed for exchanging the control messages to establish a lightpath and define T_k as the time from when a TCP session starts to when the data transfer completes.

For the biologically-inspired wavelength allocation methods, we set the parameters to be $k^{(P)} = 1$, $D = 0.7$, $P = 1$, $\alpha = 1$, and $S_1^{(0)} = 8$. For the arrivals of data transfer requests, we prepare two scenarios:

(1) Arrial rate of data transfer request is set to be 13.2 request/s for [0s-100s, 900-1500s], and increase the arrival rate to be 32.4 requests/s for [100s -900s] (Figure 5(a));

(2) Arrival rate is set to $\beta \times 10.1$ request/s . The β is the integer number between 1 to 5 and is selected randomly for every 100s. Resulting arrival rate depending on the time is shown in Figure 5(b).

For comparison purpose, we prepare the fixed wavelength allocation with seven wavelengths for the path switching plane (and thus one wavelength for the packet switching plane). In addition, we prepare the pre-calculated wavelength allocation (denote "pre-calculated") by assuming that the arrival rate is known beforehand. Given the arrival rate, we conduct the simulation and calculate the optimal wavelength allocation that achieves minimum latency. Note that "pre-calculated" changes the wavelength allocation based on the changes of arrival rate, not based on the current network conditions such as buffer utilization and/or blocking rate of lightpath establishments. We also uses threshold-based wavelength allocation method presented in [6]. In the threshold-based method, the average queue length of buffer is retrieved every 30 seconds, while

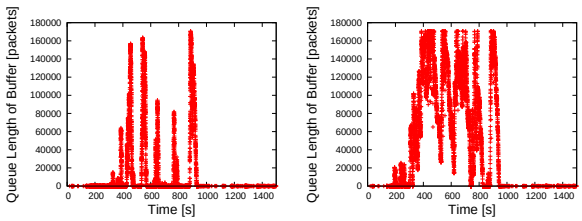

(a) Pre-calculated (b) Fixed

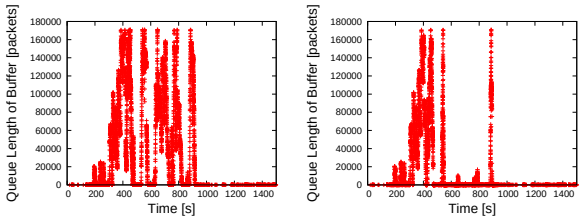

(c) Threshold-based (d) Biologically-inspired

Figure 6 Time variation of queue length : Scenario 1

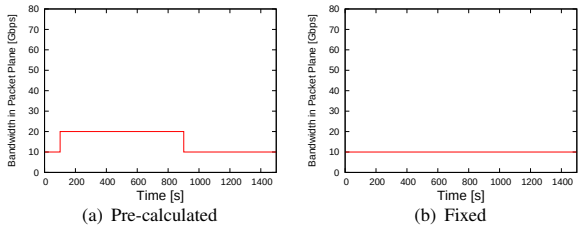

(a) Pre-calculated (b) Fixed

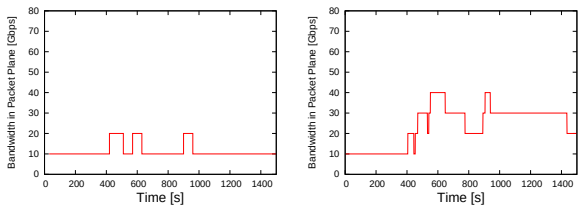

(c) Threshold-based (d) Biologically-inspired

Figure 7 Time variation of the bandwidth in the packet switching plane : Scenario 1

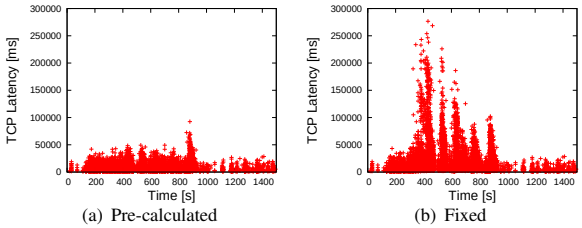

(a) Pre-calculated (b) Fixed

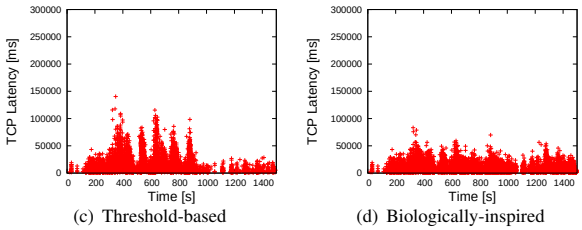

(c) Threshold-based (d) Biologically-inspired

Figure 8 Latency of TCP connections : Scenario 1

the biologically-inspired wavelength allocation method updates the values of equations at every second.

4.2 Simulation results and discussions

4.2.1 Scenario 1

Figure 6 shows the actual queue length of the buffer in the IP router. We observe that the queue length with threshold-based wavelength allocation method and biologically-inspired wavelength allocation method is less than that with the fixed wavelength allocation method (Fig 6(a)) . The queue length with the pre-calculated wavelength allocation (Fig 6(a)) is less than the biologically-inspired

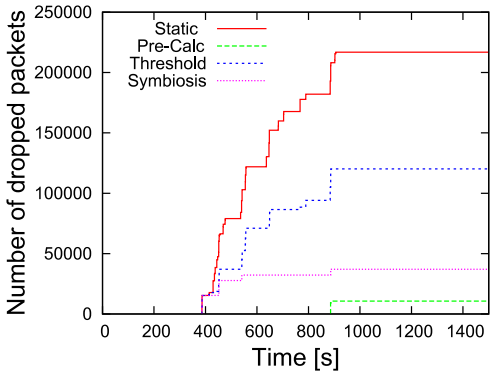

Figure 9 Accumulated number of dropped packets: Scenario 1

Table 3 Latency by wavelength allocation methods: Scenario 1

	Fixed	Threshold	Biologically-inspired	Pre-calculated
Latency (overall)	6407 [ms]	3645 [ms]	2577 [ms]	2409 [ms]
Latency (packet switching plane)	25133 [ms]	14979 [ms]	9480 [ms]	8871 [ms]

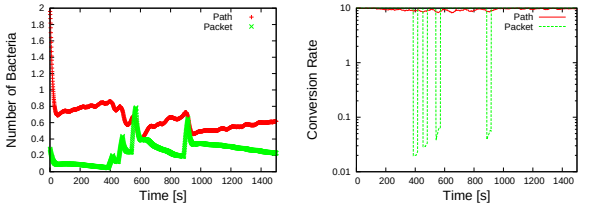

(a) Time variation of # of bacteria (b) Time variation of conversion rate

Figure 10 Behavior of biological symbiosis model : Scenario 1

wavelength allocation method, but the difference is marginal. To see how four wavelength allocation methods work, we show the time variation of bandwidth allocated for the packet switching plane in Figure 7. Both the threshold-based wavelength allocation method (Figure 7(c)) and the biologically-inspired wavelength allocation method (Figure 7(d)) adaptively changes the bandwidth for the packet switching plane. The bandwidth allocation of biologically-inspired wavelength allocation is close to the pre-calculated wavelength allocation.

Figure 8 shows the latency of TCP connections that are transferred through the packet switching plane. X-axis represents the time when a TCP connection finishes and Y-axis represent the latency of the TCP connection. Since the threshold-based and biologically-inspired wavelength allocation method decreases the average queue length during the higher arrival rate, the latency of TCP connection is greatly reduced, which in turn decreases the average latency in the path/packet integrated networks.

Figure 9 shows the accumulated number of dropped packets for each wavelength allocation method. Note that no packet loss occurs in the case of the pre-calculated wavelength allocation. The biologically-inspired wavelength allocation method takes the second smallest number of packet loss.

We next investigate the biologically-inspired wavelength allocation method in detail. To understand the behaviors of biologically-inspired wavelength allocation method, we show the time variation of number of bacteria in Figure 10(a) and the conversion rate in Figure 10(b). We observe that when the conversion rate in the packet

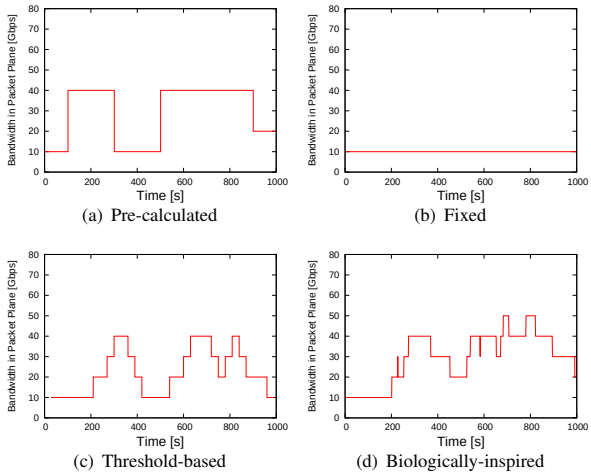

(a) Pre-calculated (b) Fixed

(c) Threshold-based (d) Biologically-inspired

Figure 11 Time variation of the bandwidth in the packet switching plane : Scenario 2

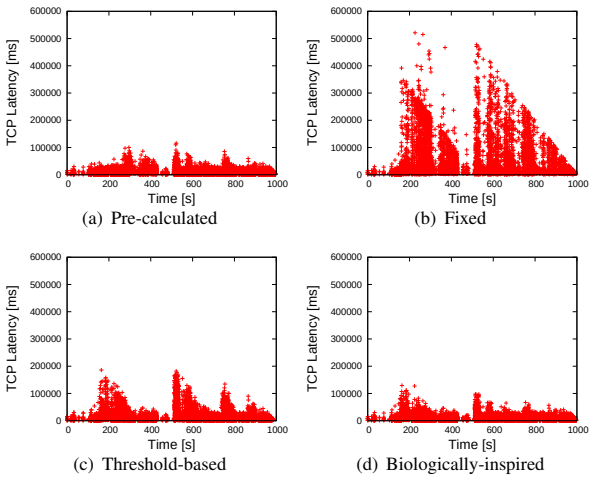

(a) Pre-calculated (b) Fixed

(c) Threshold-based (d) Biologically-inspired

Figure 12 Latency of TCP connections : Scenario 2

switching plane is drastically decreased, the number of bacteria that corresponds to the path switching plane is drastically increased. This is because the biological symbiosis model allocates the wavelength resources effectively when the traffic load on the path switching plane and the packet switching plane is not balanced. Table 3 shows the overall latency in path/packet integrated networks and the latency of data transfers that uses the packet switching plane. Note that when the lightpath establishment succeeds, the latency is around 180 [ms] since the data itransfer time with the bandwidth of lightpath. From Table 3, we observe that the biologically-inspired wavelength allocation method makes the latency to be low.

4.2.2 Scenario 2

The arrival rate used in Scenario 2 is shown in Figure 5(b). We first show the results of bandwidth allocated for the packet switching plane (Figure 11), latency of TCP connections (Figure 12), and accumulated number of dropped packets (Figure 13). The simulation results of Scenario 2 are almost the same as the simulation results of Scenario 1; the biologically-inspired wavelength allocation method makes latency low. These results show that the biologically-inspired wavelength allocation model achieves adaptive wavelength allocation against the changes of network environments.

5. Conclusion

The main advantage of the path/packet integration is to enjoy

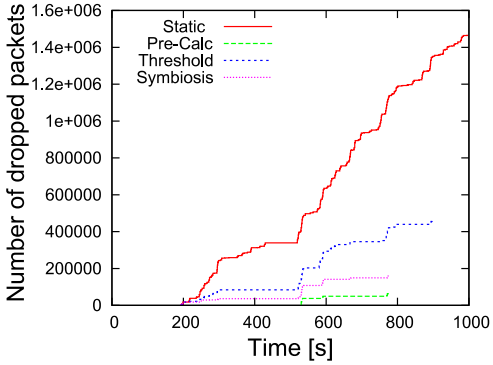

Figure 13 Accumulated number of dropped packets: Scenario 2

Table 4 Latency by wavelength allocation methods: Scenario 2

	Fixed	Threshold	Biologically-inspired	Pre-calculated
Latency (overall)	14731 [ms]	7462 [ms]	4789 [ms]	5124 [ms]
Latency (packet switching plane)	53856 [ms]	16723 [ms]	9974 [ms]	9064 [ms]

strengths of both packet switching paradigm and circuit switching paradigm. However, depending on the network condition, the amount of wavelengths allocated for networks should be changed to achieve the minimum latency. In this paper, we developed a biologically-inspired wavelength allocation method that dynamically allocates wavelengths to path/packet integrated networks. Our method is based on a biological symbiosis model that explains co-existing and co-working of two types of bacterial strains in biological systems. The results showed that biologically-inspired wavelength allocation method achieves a nealy 40% reduction of the latency from threshold-based dynamic wavelength allocation method.

References

[1] H. Zang, J. P. Jue, L. Sahasrabuddhe, R. Ramamurthy, and B. Mukherjee, "Dynamic lightpath establishment in wavelength-routed WDM networks," *IEEE Communications Magazine*, pp. 100–108, Sept. 2001.

[2] M. Kodialanm and T. V. Lakshman, "Intergrated dynamic IP and wavelength routing in IP over WDM networks," in *Proceedings of IEEE INFOCOM*, pp. 358–366, Apr. 2001.

[3] M. Veeraraghavan, X. Zheng, W. Feng, H. Lee, E. K. Chong, and H. Li, "Scheduling and transport for file transfers on high-speed optical circuits," *Journal of Grid Computing*, vol. 1, pp. 395–405, Dec. 2003.

[4] S. Lin and N. McKeown, "A simulation study of IP switching," in *Proceedings of ACM SIGMCOM1997*, pp. 15–24, Sept. 1997.

[5] M. Ohashi, S. Arakawa, and M. Murata, "Implementation and evaluation of fast lightpath setup method in wavelength-routed WDM networks," in *Proceedings of SPIE APOC 2006*, vol. 6354, pp. 63541V–1 – 63541V–9, Sept. 2006.

[6] 筒井, 荒川, 村田, "WDM を用いたパケット／パス光統合ネットワークの転送遅延の評価," **電子情報通信学会技術研究報告** (PN2009-26), pp. 29–34, Oct. 2009.

[7] T. Yomo, W.-Z. Xu, and I. Urabe, "Mathematical model allowing the coexistence of closely related competitors at the initial stage of evolution," *Researched on Population Elocogy*, vol. 38, no. 2, pp. 239–247, 1996.

[8] H. Jiang and C. Dovrolis, "Passive estimation of TCP round-trip times," *ACM SIGCOMM Computer Communication Review*, vol. 32, pp. 75–88, July 2002.